Choi et al. Journal of Analytical Science and Technology (2015) 6:29
DOI 10.1186/s40543-015-0068-z

Journal of Analytical Science and Technology
a SpringerOpen Journal

RESEARCH ARTICLE Open Access

Comparative studies on manual and automatic backbone chemical shift assignments of $^{2}H/^{13}C/^{15}N$-labeled Ube2g1

Yun-Seok Choi[1†], Eun-Hee Kim[2†] and Kyoung-Seok Ryu[1,2*]

Abstract

Background: Ube2g1, one of human E2 enzymes, possesses an additional acidic loop in the vicinity of the active Cys90 residue. The presence of the backbone chemical shifts (bCSs) is essential for various NMR studies of Ube2g1. Triple resonance experiments for the bCSs assignment of $^{13}C/^{15}N$-labeled Ube2g1 were not efficient due to the relatively high molecular size (more than 20 kDa).

Methods: $^{2}H/^{13}C/^{15}N$-labeled Ube2g1 was prepared to increase the T2 relaxation time, and then the TROSY-based triple resonance spectra were recorded with ^{2}H decoupling. After the bCSs of Ube2g1 were assigned manually, the resulting bCSs were compared with those from two different automatic assignment programs. The AutoAssign program that utilizes only the peak lists of the NMR spectra accomplished 69 % assignment of the bCSs. On the other hand, the RASPnmr program requires the additional reference CSs that can be predicted from a relevant PDB coordinate. The homologous models of Ube2g1 were generated by various modeling programs, and then their CSs were predicted by using the SHIFTX2 program.

Results: The implementations of the predicted bCSs into the RASPnmr analysis resulted in complete and accurate assignment of the bCSs of $^{2}H/^{13}C/^{15}N$-labeled Ube2g1.

Conclusions: The reference bCSs calculated from various homologous models of Ube2g1 enabled the automatic bCSs assignment process by the RASPnmr program, and a similar application will be possible for the bCS assignments of other proteins.

Keywords: Chemical shift assignment; Deuteration; Homologous modeling; NMR; RASPnmr; SHIFTX2; Ube2g1

Background

Ubiquitylation is one of important cellular modifications and regulates varieties of biological functions, such as cell cycle control, transcriptional regulation, and DNA repair (Hershko and Ciechanover 1998). During the ubiquitylation, E2 enzyme accepts a ubiquitin from E1 enzyme and then transfers the ubiquitin to a substrate with the assistance of E3 enzyme. More than several dozens of E2 enzyme have been identified in humans, and E2 enzymes have structural diversity for their own specific ubiquitylation activities. Human ubiquitin-conjugating enzyme E2 G1 (Ube2g1) is mainly expressed in skeletal muscle and testis and is moderately expressed in 15 other tissues (Watanabe et al. 1996; Lin and Wing 1999). Interestingly, Ube2g1 has a distinct acidic loop (residues 97–109) in the vicinity to the active Cys90 and the mutation of the acidic loop resulted in the impaired K48 ubiquitylation activity (Choi et al. 2015). Ube2r1 (human Cdc34) and Ube2g2 are another E2 enzymes that have a similar acidic loop. It has been reported that the acidic loops of Cdc34 and Ube2g2 also play an important role during their specific K48 ubiquitylation reactions (Petroski and Deshaies 2005; Li et al. 2007). Especially, Ube2g2 has a particular K48 ubiquitylation mechanism in the presence of gp78 (E3 enzyme), in which poly-ubiquitin chain is pre-assembled at the catalytic Cys residue (Li et al. 2007).

* Correspondence: ksryu@kbsi.re.kr
†Equal contributors
[1]Department of Bio-Analytical Science, University of Science and Technology, 217 Gajeong-Ro, Yuseong-Gu, Daejeon 305-333, South Korea
[2]Protein Structure Group, Korea Basic Science Institute, 162 Yeongudanji-Ro, Ochang-Eup, Cheongwon-Gu, Cheongju-Si, Chungcheongbuk-Do 363-883, South Korea

Table 1 The backbone chemical shift values of $^{2}H/^{13}C/^{15}N$-labeled Ube2g1

Residue		H	N	CA	CB	CO	Residue		H	N	CA	CB	CO	Residue		H	N	CA	CB	CO
G	−2	–	–	–	–	–	A	57	9.503	127.2	49.86	22.54	175.0	H	115	7.069	124.1	54.72	30.58	174.5
S	−1	–	–	–	–	–	H	58	9.315	120.1	52.62	33.37	175.5	T	116	8.170	107.6	59.01	72.11	175.7
M	1	–	–	55.90	31.68	177.0	L	59	8.932	126.4	52.99	45.07	174.9	V	117	7.765	117.9	66.56	30.33	177.7
T	2	8.119	115.8	62.90	69.33	175.2	T	60	8.502	120.1	60.71	69.57	174.5	E	118	8.451	120.8	60.28	28.72	177.2
E	3	8.213	123.2	56.89	29.65	176.8	F	61	9.757	129.0	55.36	39.99	172.5	T	119	7.472	114.9	66.20	68.51	178.1
L	4	8.194	121.9	55.74	41.56	179.0	P	62	–	–	61.28	31.20	177.6	I	120	7.662	120.8	65.11	37.51	177.1
Q	5	8.518	120.3	58.45	27.58	178.6	K	63	8.643	117.6	58.02	30.87	177.6	M	121	8.129	117.8	56.63	29.76	178.6
S	6	8.549	114.3	60.53	62.96	175.9	D	64	8.663	114.8	51.79	37.92	176.2	I	122	8.310	119.6	64.42	36.57	179.5
A	7	7.427	124.7	55.00	17.45	179.5	Y	65	7.540	123.9	57.44	39.46	173.8	S	123	7.513	117.7	62.27	–	177.1
L	8	7.559	118.2	57.68	40.77	180.3	P	66	–	–	63.76	31.51	175.5	V	124	8.253	124.3	65.78	30.33	176.9
L	9	7.987	120.3	57.48	41.19	179.3	L	67	9.231	126.0	57.54	39.98	177.1	I	125	8.402	121.4	65.36	36.25	179.2
L	10	8.319	120.9	58.17	41.01	179.0	R	68	6.707	114.6	51.91	32.00	171.5	S	126	8.008	114.4	61.36	62.69	176.8
R	11	8.246	118.7	59.54	28.98	179.6	P	69	–	–	–	–	–	M	127	7.840	121.8	57.21	30.55	178.5
R	12	7.777	119.9	58.92	29.21	179.1	P	70	–	–	60.94	30.52	175.1	L	128	7.521	120.8	57.13	39.30	176.5
Q	13	8.841	120.0	59.17	27.27	179.4	K	71	7.635	115.5	54.24	33.63	175.3	A	129	7.300	118.2	53.21	19.03	177.8
L	14	8.524	122.1	57.55	40.16	178.5	M	72	8.903	123.9	54.10	35.54	172.5	D	130	7.988	117.4	51.59	41.66	171.1
A	15	7.681	120.7	54.63	17.17	181.5	K	73	8.496	128.2	53.74	36.00	176.7	P	131	–	–	62.34	30.49	174.7
E	16	8.288	118.7	58.83	28.60	179.2	F	74	9.856	126.5	60.52	38.48	175.7	N	132	8.756	120.0	52.39	39.24	176.4
L	17	7.725	120.3	56.89	40.93	178.6	I	75	9.188	124.5	60.12	36.30	177.5	G	133	8.543	112.1	45.15	–	173.9
N	18	7.801	115.4	54.72	38.64	176.6	T	76	7.493	119.1	62.88	70.02	173.7	D	134	8.088	120.2	55.10	40.58	176.0
K	19	7.638	119.6	57.57	32.35	176.1	E	77	8.430	127.3	57.58	28.92	175.2	S	135	7.943	114.2	55.17	62.81	172.3
N	20	7.778	117.3	50.71	39.33	170.8	I	78	8.579	124.0	60.03	40.20	171.0	P	136	–	–	62.62	31.67	175.8
P	21	–	–	63.18	31.45	177.3	W	79	6.210	128.0	54.53	30.44	174.3	A	137	8.065	125.8	52.67	19.43	177.5
V	22	8.366	122.4	60.77	32.50	175.9	H	80	9.352	128.3	55.77	33.58	172.9	N	138	7.734	115.7	50.57	36.89	176.1
E	23	8.346	124.6	57.57	28.90	177.4	P	81	–	–	65.07	32.49	175.9	V	139	8.585	121.6	65.06	30.75	178.0
G	24	8.346	110.0	45.38	–	173.1	N	82	11.510	117.2	53.59	39.85	172.0	D	140	7.742	122.3	57.12	40.27	177.8
F	25	7.442	114.9	55.99	41.20	173.6	V	83	7.452	120.5	60.35	32.74	175.4	A	141	6.837	122.3	53.66	15.46	179.3
S	26	8.546	114.6	56.94	65.37	172.7	D	84	8.792	126.1	53.05	41.44	178.4	A	142	8.023	118.8	55.18	17.99	178.6
A	27	8.840	124.6	50.62	23.41	175.7	K	85	8.790	121.9	58.95	31.35	177.3	K	143	7.883	120.0	59.68	31.50	178.5
G	28	8.307	107.1	44.05	–	171.0	N	86	8.780	117.5	52.81	38.07	176.0	E	144	7.896	118.7	58.69	30.26	179.1
L	29	8.361	118.0	53.97	39.98	178.3	G	87	8.445	109.2	44.75	–	174.7	W	145	8.504	120.2	60.44	–	176.9
I	30	7.412	124.6	64.49	38.13	175.7	D	88	8.395	123.6	56.10	40.05	176.1	R	146	7.757	115.7	58.51	30.48	179.1

Table 1 The backbone chemical shift values of $^{2}H/^{13}C/^{15}N$-labeled Ube2g1 *(Continued)*

D	31	9.493	121.9	52.30	43.62	176.4	V	89	8.188	123.9	63.17	31.62	175.7	E	147	8.419	116.0	57.12	30.45	177.2
D	32	8.513	124.4	56.42	40.27	176.1	C	90	8.551	130.3	57.66	27.00	173.3	D	148	8.827	122.5	53.07	40.86	177.1
N	33	8.458	114.4	53.05	38.80	174.7	I	91	6.766	115.6	58.81	40.26	176.6	R	149	8.222	125.0	59.80	29.47	177.3
D	34	8.294	121.8	52.43	41.39	175.3	S	92	8.585	120.6	62.06	–	–	N	150	8.177	111.2	52.87	38.40	174.6
L	35	8.587	125.1	55.39	41.48	175.7	I	93	7.862	119.4	63.14	37.07	172.7	G	151	7.442	110.9	44.89	–	174.2
Y	36	8.271	111.8	59.78	36.54	175.7	L	94	6.774	113.0	52.64	39.65	176.8	E	152	9.192	131.1	58.63	29.53	177.5
R	37	6.793	116.6	55.31	31.12	175.1	H	95	7.955	119.6	53.56	29.57	174.7	F	153	7.581	116.1	62.82	37.62	176.4
W	38	9.575	127.3	55.05	31.35	175.6	E	96	8.948	123.9	54.88	28.75	175.1	K	154	6.681	118.0	59.38	31.45	177.8
E	39	9.297	122.3	54.72	–	175.0	P	97	–	–	63.85	31.29	177.4	R	155	8.108	118.8	59.59	29.62	180.0
V	40	9.435	123.9	58.59	34.35	173.4	G	98	8.505	108.7	44.63	–	174.2	K	156	8.094	120.6	60.10	32.41	180.8
L	41	8.659	126.8	53.50	42.95	175.7	E	99	7.919	120.9	56.34	29.54	176.6	V	157	8.516	122.6	67.29	30.39	178.2
I	42	9.200	125.9	59.51	39.97	174.6	D	100	8.396	123.2	54.14	40.69	176.7	A	158	8.867	123.2	55.07	16.80	180.9
I	43	8.245	127.9	57.56	36.11	177.8	K	101	8.182	121.4	56.46	31.55	176.2	R	159	7.515	118.1	59.08	28.61	178.5
G	44	9.369	114.8	43.58	–	172.7	Y	102	7.945	119.1	57.22	37.34	176.5	C	160	7.666	118.9	61.60	25.70	178.3
P	45	–	–	–	–	–	G	103	8.034	109.0	45.35	–	173.8	V	161	8.912	125.7	66.68	30.83	179.3
P	46	–	–	62.52	31.29	176.4	Y	104	7.686	118.8	57.26	37.64	175.9	R	162	8.310	122.3	58.86	28.59	179.4
D	47	8.986	115.6	55.80	38.92	175.3	E	105	8.147	122.8	56.03	29.92	176.1	K	163	8.266	119.1	58.63	31.02	179.4
T	48	7.466	106.1	60.16	73.96	177.0	K	106	8.470	122.8	53.97	31.24	175.6	S	164	7.830	116.0	60.90	61.81	175.0
L	49	9.598	121.7	56.55	40.85	176.4	P	107	–	–	64.70	30.89	178.1	Q	165	7.250	121.0	56.34	27.95	177.2
Y	50	7.351	113.7	57.88	38.34	174.0	E	108	9.028	115.9	57.59	27.85	176.7	E	166	7.697	120.0	57.06	29.34	177.4
E	51	7.091	122.3	57.58	29.31	176.7	E	109	7.878	119.7	55.72	29.27	175.4	T	167	7.921	113.3	61.93	69.40	174.5
G	52	8.599	114.7	44.49	–	175.2	R	110	7.356	119.5	54.13	31.18	174.6	A	168	7.847	125.8	52.53	18.37	177.4
G	53	8.524	108.0	45.17	–	171.2	W	111	8.424	120.1	59.72	29.52	175.7	F	169	8.011	118.8	57.02	38.88	174.9
V	54	7.437	124.1	61.03	31.50	174.4	L	112	5.885	126.6	50.43	45.26	–	E	170	7.671	126.9	57.52	30.31	180.9
F	55	9.057	124.4	56.11	40.79	174.1	P	113	–	–	64.22	–	175.7							
K	56	9.290	123.9	55.09	33.10	176.1	I	114	5.597	107.4	60.18	37.30	176.6							

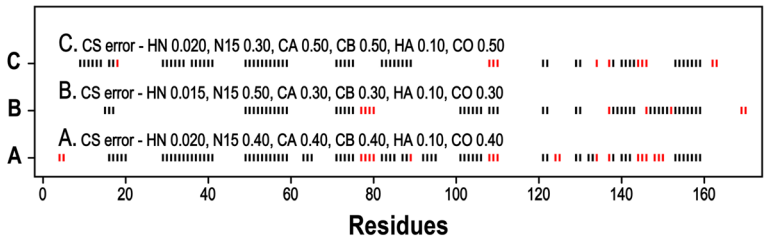

Fig. 1 Automatic bCSs assignment of $^{2}H/^{13}C/^{15}N$-labeled Ube2g1 using the AutoAssign program. The correctly and wrong assigned residues are indicated with *black* and *red bars*, respectively. The analyses using varied error values resulted in somehow different assignments. However, there was no clear variation of the assignment accuracy among the results. The analyses using the AutoAssign program accomplished overall 58 and 11 % of correct and wrong assignments compared to the manually assigned bCSs of $^{2}H/^{13}C/^{15}N$-labeled Ube2g1

The X-ray crystallography is already a well-established technique and has many advantages compared to the NMR technique for determining the three-dimensional (3-D) structure of a protein. However, most protein NMR experiments are performed in aqueous solution and thus are suitable to study the protein–protein interaction and detailed molecular dynamics of a target protein. The presence of backbone chemical shifts (bCSs) is a prerequisite of various NMR experiments to study the nature of a target protein. Here, we determined the bCSs of $^{2}H/^{13}C/^{15}N$-labeled Ube2g1 and compared the efficiency of two different automatic bCSs assignment programs, the AutoAssign (Moseley et al. 2001) and the RASPnmr (MacRaild and Norton 2014) programs.

Methods

Protein expression and purification

Human *ube2g1* gene was cloned into pGEX-4T-1 vector using BamH 1/Xho I restriction enzymes. The $^{2}H/^{13}C/^{15}N$-labeled Ube2g1 was obtained by growing *E. coli* Rosetta DE3 strain in 99 % D_2O M9 minimal media supplemented with 1 g of ^{15}N-NH_4Cl, 2 g of $^{2}H/^{13}C$-glucose, and 0.5 g of $^{2}H/^{13}C/^{15}N$-Celtone base powder (Cambridge Isotope Laboratories, Inc.). One milliliter of 2 M $MgSO_4$ and 0.1 ml of 1 M $CaCl_2$ that were prepared in 99 % D_2O solutions were appended for 1-l M9 culture. MEM vitamin (100X, SIGMA) and the trace metal D_2O solutions were prepared by re-dissolving the freeze-drying powders using 99 % D_2O solutions. The trace metal solution (200 μl) that consisted of 2 mM $CoCl_2$, 2 mM $CuSO_4$, 10 mM $FeCl_2$, 10 mM H_3BO_3, 10 mM $MnSO_4$, 5 mM Na_2MoO_4, 2 mM Na_2SeO_3, and 5 mM $ZnSO_4$ was added into 1-l M9 culture.

The GST-tagged Ube2g1 protein was purified by using Hitrap-GST affinity column (GE Healthcare). The elution fractions were concentrated, and then the GST tag was cleaved by thrombin digestion. Ube2g1 was finally purified by gel filtration column chromatography (GFC) using Superdex 75 (GE Healthcare) in buffer (pH 7.0, 50 mM HEPES, 100 mM NaCl, 1 mM DTT), and the remained GST tag in the purified Ube2g1 protein was completely removed by passing into the small volume of GST-affinity column.

NMR experiments and data analysis

Three hundred microliters of 0.8 mM $^{2}H/^{13}C/^{15}N$-Ube2g1 was prepared in a buffer (pH 7.0, 50 mM HEPES, 100 mM NaCl, 5 mM DTT, and 5 % D_2O) and then was transferred into a Shigemi tube. For the backbone chemical shift (bCS) assignment of Ube2g1, TROSY version NMR data of $^{1}H,^{15}N$-Trosy, trHNCO, trHN(CA)CO, trHNCA, trHN(CO)CA, trHN(CO)CACB, and trHNCACB was recorded at 25 °C using Bruker 900 MHz NMR spectrometer equipped with a cryogenic

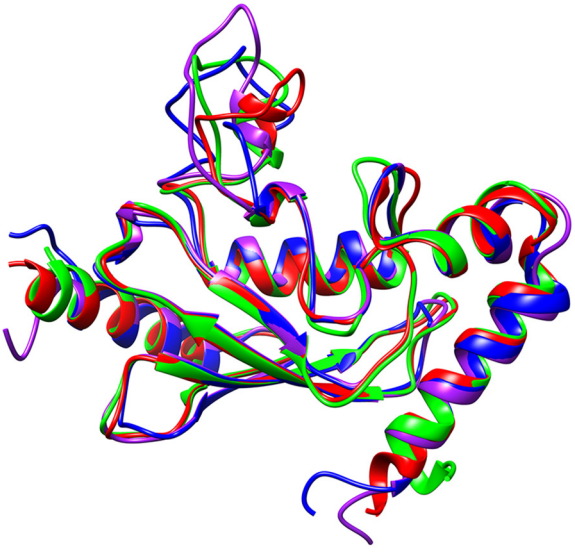

Fig. 2 Four homologous structures of Ube2g1 are overlaid. The homologous models were calculated using the Web-based modeling programs; I-TASSER (*red*), IntFOLD2 (*green*), Phyre2 (*blue*), RaptorX (*purple*). The structured regions of Ube2g1 are well superposed, but the unstructured regions (the N/C-terminal and the acidic loop parts) are not

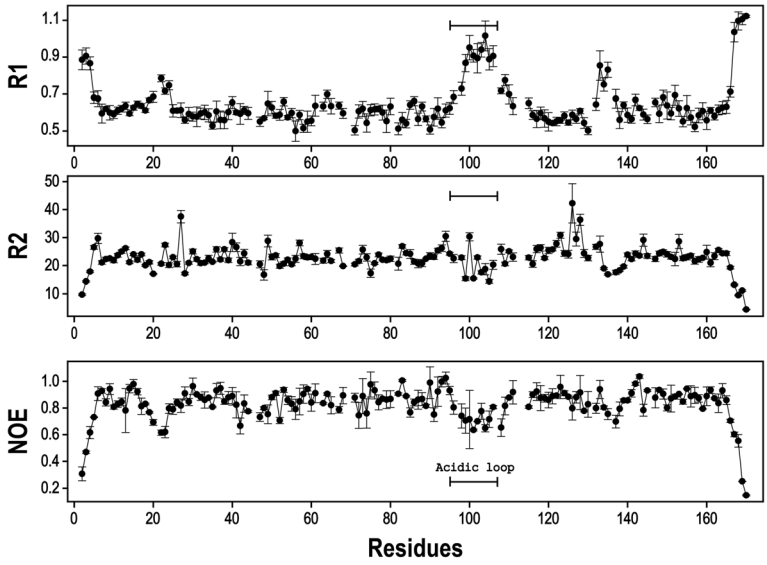

Fig. 3 The R1, R2, and ^{1}H, ^{15}N heteronuclear NOE (NOE) values of Ube2g1. The ^{15}N-relaxation data of $^{2}H/^{13}C/^{15}N$-labeled Ube2g1 were measured using 800 MHz NMR at 30 °C. The ^{15}N-relaxation data of the amide bonds show that the acidic loop region (i.e., residues 97–109) is more flexible compared to the other structured regions of Ube2g1

probehead. All data were processed using the NMRPipe program (Delaglio et al. 1995), and the resulting NMR spectra were analyzed using the SPARKY program (Goddard and Kneller).

The automatic assignments of bCSs were done using two different programs, the AutoAssign (Moseley et al. 2001) and the RASPnmr (MacRaild and Norton 2014). The second one required an additional input of the reference CS values that can be predicted from the Protein Data Bank (PDB) coordinate. The four different homologous model structures of Ube2g1 were generated *via* the Web-based analysis programs (I-TASSER (Yang et al. 2015), IntFOLD2 (McGuffin et al. 2015), Phyre2 (Kelley et al. 2015), RaptorX (Kallberg et al. 2014)). The SHIFTX2 program (Han et al. 2011) calculated the reference CSs of $^{2}H/^{13}C/^{15}N$-Ube2g1 using these four different PDB structures. All visualization of the PDB structures was done using the Chimera program (Pettersen et al. 2004).

Results and discussion

Although Ube2g1 consists of 170 amino acids (molecular weight, ~20 kDa), its apparent molecular size that includes the effect of protein shape seemed to be much higher. The molecular size of Ube2g1 was roughly estimated to be ~25 kDa during the final GPC purification. The triple resonance experiments using $^{13}C/^{15}N$-labeled sample were not efficient due to the short T2 relaxation time, and thus we prepared per-deuterated Ube2g1 protein by growing *E. coli* cell in D_2O-M9 media containing $^{2}H/^{13}C$-glucose and ^{15}N-NH_4Cl. The deuterium-labeled protein can increase the T2 relaxation time of the amide protons, due to the smaller gyromagnetic ratio of deuterium compared to that of proton (4.065×10^7 vs. 2.675×10^8 rad s^{-1} T^{-1}). Three pairs of NMR spectra that showed a sequential connectivity between two residues were recorded with ^{2}H decoupling, (i) trHNCO and trHN(CA)CO, (ii) trHNCA and trHN(CO)CA, and (iii) trHN(CO)CACB and trHNCACB. The assignment of

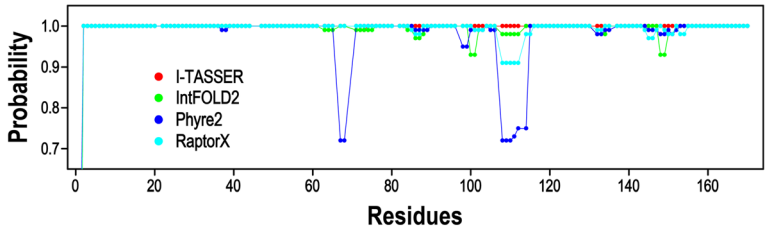

Fig. 4 The summaries of the automatic assignment results from the RASPnmr analysis. The reference CSs were calculated for the model structures (I-TASSER, IntFOLD2, Phyre2, and RaptorX) using the SHIFTX2 program, and then the predicted CSs values were implemented to the RASPnmr analyses. The probabilities of the correctly assigned residues by the RASPnmr program are shown for the different reference CS values

backbone chemical shifts (bCSs) of $^{2}H/^{13}C/^{15}N$-Ube2g1 (H_N, N, C_α, C_β, and C_{CO}) was manually performed. The bCSs of most residues were completely assigned except for those of Met1. The C_α, C_β, and C_{CO} of Pro45 and Pro69 could not be assigned because of the presence of consecutive Pro46 and Pro70, respectively (Table 1). The automatic bCS assignment can provide a great convenience to manual assignment that is a time-consuming and tedious process. We first tried to assign the bCS of Ube2g1 using the AutoAssign program that utilizes the peak lists of all pairs of NMR spectra (Moseley et al. 2001). During the analysis, the error values were varied for each different types of CSs (H_N, N, C_α, C_β, and C_{CO}). Although the variation of error values caused different assignments, any clear improvement in the assignment results was not identified for the different analyses (Fig. 1). Unfortunately, this automatic assignment using the AutoAssign program was not complete for the bCSs of Ube2g1. Only 58 and 11 % of the residues were correctly and wrongly assigned, respectively, and 31 % of the residues still remained to be unassigned.

To increase the efficiency of automatic assignment, we tried to use the RASPnmr program that requires additional information of the CS reference that can be calculated from the PDB coordinate of a target protein (MacRaild and Norton 2014). The RASPnmr program is capable of auto-assigning only for the residues of which the reference bCSs are present. The X-ray structure of Ube2g1 has not yet been available, and the 3-D coordinate of the truncated Ube2g1 (2AWF) is only deposited to the Protein Data Bank. There are many PDB coordinates of various E2 proteins, and thus the model structures of Ube2g1 could be readily prepared by using various homologous modeling programs. Therefore, we generated four different homologous models of Ube2g1 using the Web-based modeling programs, I-TASSER (Yang et al. 2015), IntFOLD2 (McGuffin et al. 2015), Phyre2 (Kelley et al. 2015), RaptorX (Kallberg et al. 2014), to take account of the effects from wrong CS references during the RASPnmr analyses. These programs can produce the coordinate also for the unstructured regions of Ube2g1 (the N/C-terminal parts and the acidic loop). The model structures of Ube2g1 could be well superimposed, except for the flexible regions including the N/C-terminal parts and the acidic loop (Fig. 2). The presence of the flexible parts in these homologous models of Ube2g1 was also confirmed by the measured ^{15}N-relaxation data (T1, T2, and $^{1}H,^{15}N$-heteronuclear NOE values) (Fig. 3). The estimated rotational correlation times using the T1/T2 ratios (Kay et al. 1989) were roughly 12 to 14 ns for the rigid part of Ube2g1, which indicates the molecular size of Ube2g1 is larger than 20 kDa. The theoretical CS values of the model structures were calculated by using the SHIFTX2 program (Han et al. 2011), and then were implemented to the automatic assignments of the RASPnmr program as the bCSs reference. Indeed, the automatic assignments using the RASPnmr program accomplished almost complete and accurate assignment of the Ube2g1 bCSs (Fig. 4). Although four different sets of the reference bCSs resulted in slightly different and wrong assignments during the RASPnmr analyses, the analyses resulted in almost identical and correct auto-assignments. The probabilities of the correct assignments using the Phyre2 model were lower in the acidic loop region than those using the other models, but the values were still higher than 70 %. There are many programs to predict the homologous model of protein structure, and they utilize their own specific algorism. The homologous models of Ube2g1 seem to be accurate for the E2-core domain, but those of the unstructured parts vary with the algorisms of the modeling program (Fig. 2). Nevertheless, the presence of homologous 3-D structure enables an efficient performance of the RASPnmr program and thus likely accelerates the tedious bCS assignment that is very slow especially for a larger protein.

Conclusions

The perdeuteration of Ube2g1 protein increased the T2 relaxation time and made it possible to record various pairs of triple resonance NMR spectra that are used for the bCS assignment. The calculation of the reference bCSs using the SHIFTX2 program based on the homologous models of Ube2g1 enabled the highly efficient automatic bCS assignment by using the RASPnmr program.

Competing interests

The authors declare that they have no competing interests.

Authors' contributions

KSR designed the whole work and wrote the manuscript. The sample preparation, NMR acquisition, and analyses of data have been done by YSC and EHK. All authors read and approved the final manuscript.

Acknowledgements

This study was also supported by KBSI Grant C35938 (to K. S. Ryu).

Received: 6 July 2015 Accepted: 27 September 2015
Published online: 16 October 2015

References

Choi YS, Lee YJ, Lee SY, Shi L, Ha JH, Cheong HK, et al. Differential ubiquitin binding by the acidic loops of Ube2g1 and Ube2r1 enzymes distinguishes their Lys-48-ubiquitylation activities. J Biol Chem. 2015;290:2251–63.

Delaglio F, Grzesiek S, Vuister GW, Zhu G, Pfeifer J, Bax A. NMRPipe: a multidimensional spectral processing system based on UNIX pipes. J Biomol NMR. 1995;6:277–93.

Goddard T. D. & Kneller D. G. SPARKY 3, University of California, San Francisco. (https://www.cgl.ucsf.edu/home/sparky/).

Han B, Liu Y, Ginzinger SW, Wishart DS. SHIFTX2: significantly improved protein chemical shift prediction. J Biomol NMR. 2011;50:43–57.

Hershko A, Ciechanover A. The ubiquitin system. Annu Rev Biochem. 1998;67:425–79.

Kallberg M, Margaryan G, Wang S, Ma J, Xu J. RaptorX server: a resource for template-based protein structure modeling. Methods Mol Biol. 2014;1137:17–27.
Kay LE, Torchia DA, Bax A. Backbone dynamics of proteins as studied by 15 N inverse detected heteronuclear NMR spectroscopy: application to staphylococcal nuclease. Biochem. 1989;28:8972–9.
Kelley LA, Mezulis S, Yates CM, Wass MN, Sternberg MJ. The Phyre2 web portal for protein modeling, prediction and analysis. Nat Protoc. 2015;10:845–58.
Li W, Tu D, Brunger AT, Ye Y. A ubiquitin ligase transfers preformed polyubiquitin chains from a conjugating enzyme to a substrate. Nature. 2007;446:333–7.
Lin H, Wing SS. Identification of rabbit reticulocyte E217K as a UBC7 homologue and functional characterization of its core domain loop. J Biol Chem. 1999;274:14685–91.
MacRaild CA, Norton RS. RASP: rapid and robust backbone chemical shift assignments from protein structure. J Biomol NMR. 2014;58:155–63.
McGuffin LJ, Atkins JD, Salehe BR, Shuid AN, Roche DB, Roche DB. IntFOLD: an integrated server for modelling protein structures and functions from amino acid sequences. Nucleic Acids Res. 2015;43(W1):W169–73.
Moseley HN, Monleon D, Montelione GT. Automatic determination of protein backbone resonance assignments from triple resonance nuclear magnetic resonance data. Methods Enzymol. 2001;339:91–108.
Petroski MD, Deshaies RJ. Mechanism of lysine 48-linked ubiquitin-chain synthesis by the cullin-RING ubiquitin-ligase complex SCF-Cdc34. Cell. 2005;123:1107–20.
Pettersen EF, Goddard TD, Huang CC, Couch GS, Greenblatt DM, Meng EC, et al. UCSF Chimera–a visualization system for exploratory research and analysis. J Comput Chem. 2004;25:1605–12.
Watanabe TK, Kawai A, Fujiwara T, Maekawa H, Hirai Y, Nakamura Y, et al. Molecular cloning of UBE2G, encoding a human skeletal muscle-specific ubiquitin-conjugating enzyme homologous to UBC7 of C. elegans. Cytogenet Cell Genet. 1996;74:146–8.
Yang J, Yan R, Roy A, Xu D, Poisson J, Zhang Y. The I-TASSER Suite: protein structure and function prediction. Nat Methods. 2015;12:7–8.